Epitaxial orientations of *para*-sexiphenyl platelets grown on alkali halide (001) surfaces

Detlef-M. Smilgies[1,*] and Edward J. Kintzel, Jr.[2]
[1]*Cornell High-Energy Synchrotron Source (CHESS), Cornell University, Ithaca, New York 14853, USA*
[2]*Department of Physics and Astronomy, Western Kentucky University, Bowling Green, Kentucky 42101, USA*
(Received 5 September 2008; revised manuscript received 15 May 2009; published 12 June 2009)

Thin film growth of simple aromatic molecules has been researched intensely in recent years in the burgeoning field of organic electronics. Film growth for simple rodlike molecules on the atomically well-defined and nonreactive alkali halide (001) surfaces also constitutes an archetypical model system for the study of molecular epitaxy. We have observed a surprising variety of preferential orientations of *para*-sexiphenyl platelets on a series of alkali halide surfaces with lattice constants ranging from 4.6 to 6.6 Å. We present a metric that helps to classify the dominant epitaxial orientations and allows us to predict epitaxial orientations on other rocksalt-type substrates, and we identified surface corrugation as the driving force for these preferred relative orientations.

DOI: 10.1103/PhysRevB.79.235413 PACS number(s): 68.55.am, 68.35.−p, 61.05.C−

I. INTRODUCTION

Single-crystalline organic materials offer the potential of much improved transport properties compared to polycrystalline material. Thus the growth of thin films of simple aromatic molecules has been studied intensely in the rapidly evolving field of organic electronics.[1] In particular, the simple rodlike molecule *para*-sexiphenyl (PSP) has been the target of a number of studies based on its electro-optical properties and potential use in organic light-emitting devices.[2–13]

Growth studies of PSP on alkali halide surfaces have revealed a series of epitaxial phases with two distinct orientations of the molecule relative to the substrate and associated morphologies of the resulting microcrystallites: platelets of standing molecules and several types of needles featuring lying molecules.[2–12] Despite their different habits and crystallographic orientations, all the observed crystallites on the alkali halide substrates feature the PSP bulk structure.

Predominance of one of these epitaxial phases can be achieved by carefully choosing the growth parameters.[2–12] It has been demonstrated that transport properties and optical efficiency of the molecular films are much improved over polycrystalline films if such epitaxial structures are sandwiched between electrodes after dissolving the substrate.[2]

Apart from the technological relevance for optoelectronic devices, the growth of PSP on alkali halide surfaces constitutes an archetypical model system for studying molecular epitaxy of simple rodlike molecules. Toward this goal, we have studied the in-plane orientation of PSP platelets on a series of alkali halide substrates covering a lattice constant range from 4.64 to 6.60 Å. In the following we will focus on preferential epitaxial orientations found for the PSP platelets which grow in the PSP bulk structure.[5,14]

II. EXPERIMENTAL

The PSP bulk structure consists of smectic-crystalline planes of close-packed rodlike molecules parallel to the PSP (001) crystallographic planes. The molecular lattice is monoclinic with space group $p2_1/a$ and lattice parameters $a=8.091$ Å, $b=5.535$ Å, $c=26.3$ Å, and $\beta=98°$ comprising two molecules per unit cell.[14] Epitaxially deposited films on alkali halide substrates feature three-dimensional crystallites with the PSP bulk structure but different epitaxial growth planes and different habits, such as platelets and different kinds of needles.[2–12]

In the platelet phase the molecular (001) planes are parallel to the substrate surface, i.e., PSP(001)‖substrate(001). Atomic force microscopy (AFM) revealed a terrace pattern with step heights corresponding to the PSP *c* value, as shown in Fig. 1. Figure 2 provides a partial side view onto the PSP long molecular axes in the *a*-*c* plane. Below the side view, a view at the bottom of the first molecular layer is provided. The terminal hydrogen atoms (white) are in closest contact with the substrate. The corresponding H atoms in both views are connected by dash-dotted lines. The lattice formed by the terminal H atoms is centered rectangular with lattice constants *a* and *b* from the bulk.[5]

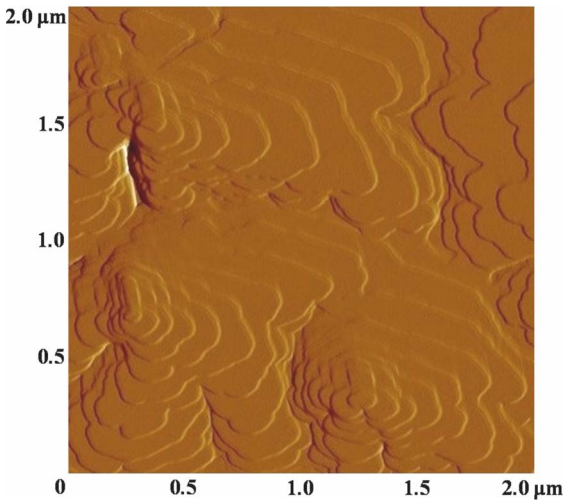

FIG. 1. (Color online) Tapping mode AFM image of PSP platelets formed on KCl (001). Size of the image is 2 μm by 2 μm. Scan direction was parallel to the substrate [100] direction. Adjacent terraces feature height differences of 26 Å in good agreement with the PSP *c* value. Terraces display irregular shapes with rounded edges.

 ©2009 The American Physical Society

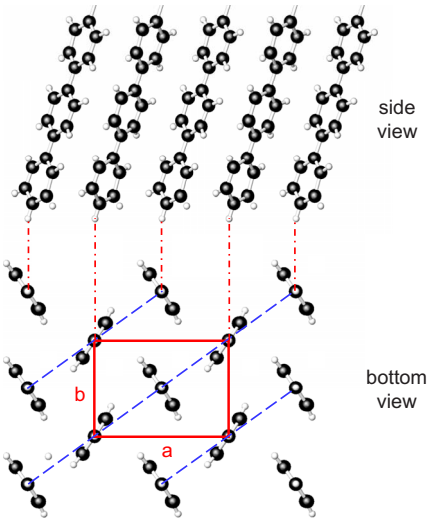

FIG. 2. (Color online) Partial side view and bottom view of a PSP layer at the substrate interface. The atoms in closest contact to the surface are the terminal hydrogen atoms (white, connected with dash-dotted lines between the views). The centered-rectangular unit cell of the terminal hydrogen atoms is indicated in the bottom view. The surface lattice constants correspond to the PSP bulk lattice constants a and b. Dense molecular rows along the PSP [110] directions, marked by dashed lines, contribute to the epitaxial alignment of the PSP platelets and will be central to the further discussion.

The natural fcc (100) cleavage planes of the alkali halide surfaces feature a square surface lattice with surface lattice vectors along the [110] bulk directions and a surface lattice parameter $a_S = a_B/\sqrt{2}$, where a_B is the bulk lattice constant. The surface lattice can be viewed as the lattice of the negative halide ions with a positive alkali ion in the center of each cell.

All films were prepared at the MARTECH facility at Florida State University, as reported earlier.[7,11] PSP films were grown by sublimation on four different alkali halide substrates (with bulk lattice constants a_B given in parentheses): NaF (4.64 Å), NaCl (5.65 Å), KCl (6.32 Å), and KBr (6.60 Å). Substrates were cleaved in air and gently heated in a deposition chamber to 150 °C to remove adsorbed water vapor before deposition of the PSP molecules in high vacuum of 10^{-8} mbar. Deposition rates were monitored with a quartz-crystal monitor and adjusted to be 0.2 ± 0.05 Å/s. Deposition was maintained, until nominal five monolayers of mass thickness of organic material was adsorbed onto each individual substrate. Substrate temperatures were chosen to optimize the yield of the platelet phase,[7,11] corresponding to 125 °C (NaF), 125 °C (NaCl), 200 °C (KCl), and 125 °C (KBr) for the four substrates.

X-ray pole figure scans were obtained at CHESS G2 station using a six-circle kappa diffractometer[15] which was configured in standard four-circle geometry. A x-ray beam was split from the main wiggler beam using an x-ray transparent Be (002) Laue crystal. The side-bounced beam was collimated to 1×1 mm^2 with two pairs of collimating slits. The photon energy was 9.5 keV with a bandwidth of 0.1% as given by the mosaicity of the Be single crystal. The detector

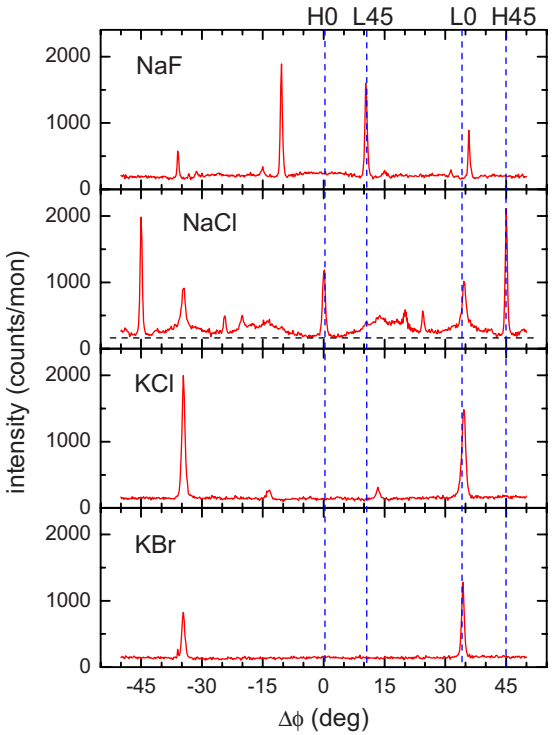

FIG. 3. (Color online) High-resolution pole figure scans of the PSP $(20\bar{3})$ Bragg reflection for PSP platelets formed during growth on NaF (001), NaCl (001), KCl (001), and KBr (001) substrates. Scans were taken with a point detector with a step size of 0.2°. The zero of the azimuth angle $\Delta\phi$ corresponds to the substrate [110] direction. Vertical dashed lines indicate the four dominant epitaxial orientations found. The horizontal dashed line in the NaCl graph indicates the background level.

arm comprised another pair of collimating 1×1 mm^2 slits and a scintillation detector.

Samples were prealigned using the reflection of a laser beam, such that the surface normal coincided with the azimuth rotation axis ϕ of the sample goniometer. Samples were then lined up in the x-ray beam with the help of the (001) and (222) substrate Bragg reflections. For pole figure scans, the PSP $(20\bar{3})$ reflection was chosen as a "search light" indicating PSP crystallites oriented with the PSP [100] direction parallel to a particular substrate azimuth angle $\Delta\phi$ which was referenced relative to the substrate [110] high-symmetry direction. The scan range was $\pm 50°$ with respect to the [110] azimuth of each substrate at a step size of 0.2°, covering a full 90° sector, as mandated by the fourfold symmetry of the substrates. Using the symmetry of the diffraction pattern, peak centers could be determined with an accuracy of 0.01°.

III. RESULTS

A. X-ray diffraction measurements

A series of azimuth scans for PSP grown on various substrates is shown in Fig. 3, using the PSP $(20\bar{3})$ searchlight reflection. Intensity maxima in the azimuth scans indicate

TABLE I. Azimuth $\Delta\phi$ values of observed preferred epitaxial orientations for PSP platelets and alkali halide (001) surfaces.

Substrate	NaF	NaCl	KCl	KBr	Bulk[a]
Bulk lattice constant (Å)	4.64	5.65	6.29	6.60	
H0: PSP[100]‖[110][b] (deg)	no[d]	0	no	no	0
L0: PSP[110]‖[110][c] (deg)	35.89	34.63	34.58	34.50	34.535
H45: PSP[100]‖[100][b] (deg)	no	45	no	no	45
L45 PSP[100]‖[100][c] (deg)	10.46	10.65	no	no	10.465
U1 (deg)	15.02	20.03	13.48		
U2 (deg)	31.35	24.44			

[a]Value calculated from the PSP bulk structure.
[b]High-symmetry configuration with PSP *a* and *b* vectors aligned.
[c]Low-symmetry configuration with PSP [110] rows aligned.
[d]Not observed.

preferential alignments of PSP platelets along distinct substrate directions. Two main epitaxial orientations were prominent: for $\Delta\phi=0°$ the PSP *a* and *b* lattice vectors are parallel to the [110] directions of the substrate (H0). In standard notation the H0 phase would be denoted PSP[100]‖substrate[110]. This high-symmetry phase was only observed on NaCl (001). The second pronounced orientation (L0) around $\Delta\phi=34.5°$ corresponds to rows of molecules along the PSP [110] direction (see Fig. 2) being parallel to the substrate [110] direction which yields a low-symmetry alignment of the molecular platelets.[5]

A second set of preferential orientations appeared at $\Delta\phi=45°$ (H45) and $\Delta\phi=10.6°$ (L45) which correspond to 45° rotated domains of the base structures. Such 45° domains are often encountered in epitaxy on square lattices. In addition we observed weak reflections that could not be rationalized in a simple way. A list of all observed preferential orientations found on the four substrates is provided in Table I.

Aligned molecular rows along PSP [110] appear to be favorable for KCl (001) and KBr (001) substrates featuring lattice constants on a similar size as the in-plane PSP *a* and *b* constants. For NaCl (001) both lined-up molecular rows and lined-up PSP high-symmetry directions seemed to be equally favored over random orientations. On NaF (001) the basic period of the substrate lattice is too small to accommodate either the L0 or H0 phase, and thus 45° domains seemed to be favored over 0° domains.

For determining the mismatch the basic substrate lattice period for the H0 (H45) phase is given by a_S ($a_S\sqrt{2}=a_B$) and the basic periods for the centered rectangular PSP lattice by either $d_{20}=a/2$ or $d_{02}=b/2$. For the L0 (L45) epitaxial phases, the distance between molecular rows given by $d_{11}=1/\sqrt{1/a^2+1/b^2}=4.59$ Å has to be matched up with the corresponding substrate period. The nearest-neighbor distance along a molecular row $d_{NN}=4.91$ Å is used to determine the mismatch in the perpendicular direction.

For the H0 (H45) phase on NaCl (001) a misfit of 1.3% (−1.5%) with respect to d_{20} ($2\,d_{02}$) are obtained. For the L0 phases on KCl (001) and KBr (001) we find 3.1% and −1.7%, respectively. It appears that growth under expansive stress (KBr) was somewhat less preferable than growth under compressive stress (KCl), as observed in our systematic growth studies.[7] Finally we got a misfit of −1.1% for the L45 phase on NaF. Note that for all of these dominant orientations the alignment appears to be correlated with a favorable lattice match in only one direction, while the lattices remain incommensurate in the perpendicular direction.

However, also other epitaxial orientations were observed than expected from simple lattice mismatch considerations. Unidentified minority phases denoted U1 and U2 were observed consistently on all substrates with the exception of KBr and are listed in Table I. These phases do not seem to fit into a known scheme. Moreover NaCl (001) features an L0 phase in addition to the H0 and H45 phases, for which no reasonable misfit below 5% can be found other than assuming unreasonable high-order commensurabilities. The high abundance of preferential orientations observed on NaCl (001) may indicate that the epitaxial orientations of the PSP platelets are only marginally stable. This is further supported by broad distributions of material in the NaCl pole figure scan beneath the sharper peaks of the L0 phase. A similar behavior was observed for the closely related molecule *para*-quaterphenyl on NaCl (001).[16]

B. Epitaxial metric

Naively one would not expect that low-symmetry and dissimilar molecular lattices would show any preferential orientation on standard high-symmetry substrates. Nonetheless, many oriented phases of molecules on inert surfaces have been reported despite the typical low symmetry of molecular lattices and their general incompatibility with common substrate lattices.[17] Haber and co-workers[18] recently found that the misfit model by Hoshino *et al.*,[19] which provides a good metric to explain atomic epitaxy in many cases, does not seem to explain the preferential orientation of PSP crystallites on KCl (001). In search of an adequate method that captures the basic physics but stopping short of using full-fledged potential models, we present a simple metric based on the essential features of the epitaxial potential.

The adatom absorption potential V_{ads} of a physisorbed atom absorbed at a surface is given by the long-range attractive van der Waals interaction and a short-range repulsion due to the overlap of electron clouds.[20–28] Due to the periodic

nature of the surface, V_{ads} can be expanded into a two-dimensional (2D) Fourier series:[20–25]

$$V_{ads}(\boldsymbol{R},z) = \sum_{\boldsymbol{G}} V_{\boldsymbol{G}}(z)\exp(i\boldsymbol{G}\boldsymbol{R}),$$

where $\mathbf{R}$ is a two-dimensional adatom position vector in the surface plane, z is the adatom position perpendicular to the surface, and $\mathbf{G}$ are the two-dimensional reciprocal lattice vectors. For the square lattices which we are concerned with, the zeroth-order term ($\mathbf{G}_{00}=0$) and the four first-order terms ($|\mathbf{G}_{10}|=|\mathbf{G}_{01}|=2\pi/a_S$) can be rewritten as[20]

$$V_{ads}(\boldsymbol{R},z) = V_{00}(z) + V_{10}(z)[\cos(\boldsymbol{G}_{10}\boldsymbol{R}) + \cos(\boldsymbol{G}_{01}\boldsymbol{R})] + \cdots,$$

where $V_{00}(z)$ is the laterally averaged adsorption potential, and its minimum z_{min} yields the optimum adatom distance from the surface plane. $V_{10}(z)$ is the first-order corrugation potential that is mainly responsible for the preferential adsorption sites inside the surface unit cell. In the case of alkali halogenide surfaces, the surface corrugation is dominated by the electron density of the negative ions.[20–24] Hence the most favorable position can be identified as the fourfold hollow in between neighboring negative ions (and thus on top of the small positive ion) and the most unfavorable position as on top of a negative ion.[23,24]

As PSP platelets maintain bulk structure,[5] we conclude that the intermolecular packing interactions are much stronger than the corrugation potential, and we can regard the packing within the molecular layer as *rigid*. Moreover, the corrugation potential is short ranged, as it is mainly determined by the short-range repulsive forces.[20–24] Thus preferential orientations of single molecular domains should primarily be determined by the *layer of point contacts* with the substrate. In our case the terminal hydrogen atoms of the PSP molecules, which form a centered rectangular lattice with the PSP bulk lattice parameters a and b (see Fig. 2), are in close contact with the surface. In this case the epitaxial potential V_{epi} of a finite circular domain of radius $R=Ma$ is given in first order by summing up all point-contact contributions of a rigid lattice within the domain:

$$V_{epi}(\varphi) = \frac{V_{10}(z_{min})}{N} \times \sum_{m,n\in\text{domain}} [\cos(\boldsymbol{G}_{10}\boldsymbol{M}_{\varphi}\boldsymbol{R}_{mn}) + \cos(\boldsymbol{G}_{01}\boldsymbol{M}_{\varphi}\boldsymbol{R}_{mn})],$$

where $\boldsymbol{M}_{\varphi}$ is a two-dimensional rotation matrix which describes the rotation angle φ between the rigid adlayer lattice $\boldsymbol{R}_{mn}$ and the substrate [110] direction. V_{epi} was normalized by the number of atoms N in the domain, in order to facilitate the comparison of results for different domain sizes.

We note that AFM images of platelets show rounded edges (see Fig. 1). Using a circular domain shape mimics this behavior. Moreover, a circular domain shape reduces extra contributions from the domain boundaries when the domain is rotated, which otherwise give rise to additional preferred orientations based on the domain shape.[29,30] The number of molecules N inside the domain can be obtained by dividing the domain area over the size of the primitive unit cell. This way we are left with a single scale factor $\varepsilon = V_1(z_{min})$ which we will set to -1 in the following, as we are primarily interested in identifying preferential orientations.

In the above ansatz we implied that the center atom ($m=0$, $n=0$) of the domain is located in a fourfold hollow position. While this works for coincidence lattices, more care has to be applied in the case of *incommensurate* lattices. For instance, we found that potential minima can turn into maxima and vice versa as a function of domain size. Furthermore, potential minima change into maxima when the center atom of a domain is moved from the fourfold hollow to the on-top position and vice versa. This means that the corrugation potential for an incommensurate layer has to be minimized for all translations $\boldsymbol{\tau}$ of the adlayer domain within the substrate surface unit cell in order to yield the proper most favorable orientation of the adlayer:

$$V'_{epi}(\varphi) = -\frac{1}{N}\min_{\boldsymbol{\tau}\in\text{uc}}\left\{\sum_{m,n\in\text{domain}} [\cos(\boldsymbol{G}_{10}[\boldsymbol{M}_{\varphi}\boldsymbol{R}_{mn}+\boldsymbol{\tau}]) + \cos(\boldsymbol{G}_{01}[\boldsymbol{M}_{\varphi}\boldsymbol{R}_{mn}+\boldsymbol{\tau}])]\right\}.$$

This apparently simple expression is computationally rather demanding. In tests using discrete grids of displacement vectors $\boldsymbol{\tau}$ within the irreducible wedge of the substrate unit cell, as given by symmetry, we found that potential minima or maxima were almost always assumed in the fourfold hollow and on-top positions. Taking into account that the potential switches sign when exchanging on-top and fourfold positions, we found that a robust metric for identifying favorable epitaxial rotations can be obtained by simply choosing

$$C(\varphi) = V^2_{epi}(\varphi).$$

Preferential epitaxial orientations show up as *maxima* of the metric $C(\varphi)$ for both the center of the domain at a fourfold hollow site or at an on-top site of the substrate. The metric has the full symmetry of the substrate lattice. This means for a simple square lattice that the angular range from 0 to 45° already contains all information. Finally we note that the metric is normalized such that it yields 1 in the case of a commensurate layer with all molecules located at the potential minima. Thus we have arrived at a convenient metric to identify favorable relative orientations of substrate and molecular lattice with the surface corrugation acting of the terminal hydrogen atoms as the driving force.

We tested the metric for a number of high-order commensurate model structures such as $\sqrt{5}\times\sqrt{5}R26.57°$, and the corresponding rotation angles were exactly reproduced. Moving on to the PSP incommensurate structures, we tested a variety of domain sizes with radii of $Ma=20a$, $50a$, and $100a$ which all yielded consistent results to within $\pm 0.1°$ in orientation and 0.02 Å in lattice constant. $M=20$ corresponds to about $N=1000$ point contacts in a single molecule domain which was used in the following.

C. Comparison to the experimental data

Strong maxima in $C(\varphi)$ were found to be associated with coincidence structures with $\varphi=0$ for the lattice constant range 5.6–5.7 Å corresponding to the high-symmetry H0

phase and φ around 34.5° for lattice constants between 6.3 and 6.5 Å for the low-symmetry L0 phase. The observed dominant diffraction spots in the azimuth scans were close to these coincidence cases. Both coincidence cases can be identified with one-dimensional alignments of the molecular lattice: in the case of NaCl (001) the molecular a lattice constant coincides with the substrate lattice a_S. In the case of KCl (001) the distance between close-packed rows of terminal H atoms is well matched with a_S.

The metric $C(\varphi)$ predicts correctly that the low-symmetry structure L0 from Table I is favorable for PSPs on KCl (001) and KBr (001). Reference 5 provided an in-depth analysis of the platelet orientation on KCl (001) using grazing-incidence diffraction, and it was observed that there is a good one-dimensional match between the spacing of PSP neighboring rows of molecules (see Fig. 1) and the spacing of the [110] rows of negative ions, which constitute the principal Fourier component of the substrate corrugation. However, there was no apparent match in the perpendicular direction. Hence we conclude that the metric is sensitive to such one-dimensional alignments.

NaCl seems to be a special case: judging by the abundance of observed orientations, the oriented phases seem to be only marginally stable which is also supported by the occurrence of broad diffraction intensity distributions in the spectra. The metric predicts correctly that in the case of NaCl the high-symmetry structure H0 with PSP [100] parallel to the substrate [110] direction is most favorable. Again the lattice misfit is only favorable in one direction: $2a$ is well matched with the surface lattice, while the other direction displays a large misfit on the order of 40% and can be considered incommensurate. Hence the alignment mechanism is again one-dimensional for the H0 type of alignment which is specific to NaCl.

For epitaxy on NaF neither the high-symmetry orientation H0 nor the low-symmetry orientation L0 yielded maxima in the metric $C(\varphi)$. This seems to be related to the fact that the NaF lattice constant is too small compared to the PSP lattice to yield favorable results in either case.

A second class of preferential orientations can be identified as 45° rotated domains, which are very common in epitaxy on square substrates but are not reproduced by our simple metric based on only the first-order components of the corrugation. However, it is well known from helium atom scattering experiments that higher Fourier components of the electron-density corrugation need to be included, in order to properly model the adsorption potential of the alkali halide (001) surfaces.[23,28]

Instead of getting into more complicated modeling of the full adatom adsorption potential,[31,32] we observe that the next-order Fourier component $V_{11}(z)$ again has four symmetry-related contributions given by the set of reciprocal lattice vectors $\{G_{11}, G_{1\bar{1}}, G_{\bar{1}1}, G_{\bar{1}\bar{1}}\}$, which is sometimes referred to as the *star of* G_{11}. Hence this contribution by itself will again result in a similar diagram as given by $C(\varphi)$, only with the lattice parameter a_s rescaled to $a_s/\sqrt{2}$ and the angular coordinates reversed (0° becomes 45° and vice versa).

In fact the (11) Fourier component by itself can be used to define a generalized metric $C_{11}(\varphi)$ (see Appendixes A and B) which we found to account for the 45° rotated structure H45 on NaCl (001). In addition, it provides a match for the observed L45 structure on NaF (001). As the NaF substrate lattice has too small a unit cell to accommodate the H0 or L0 alignments, now the (11) Fourier component of the corrugation can provide favorable arrangement. Along a similar vain, the L0 structure on NaF can be found to be favored by the (20) Fourier component of the corrugation given by an again fourfold star of G_{20} and the associated generalized metric $C_{20}(\varphi)$.

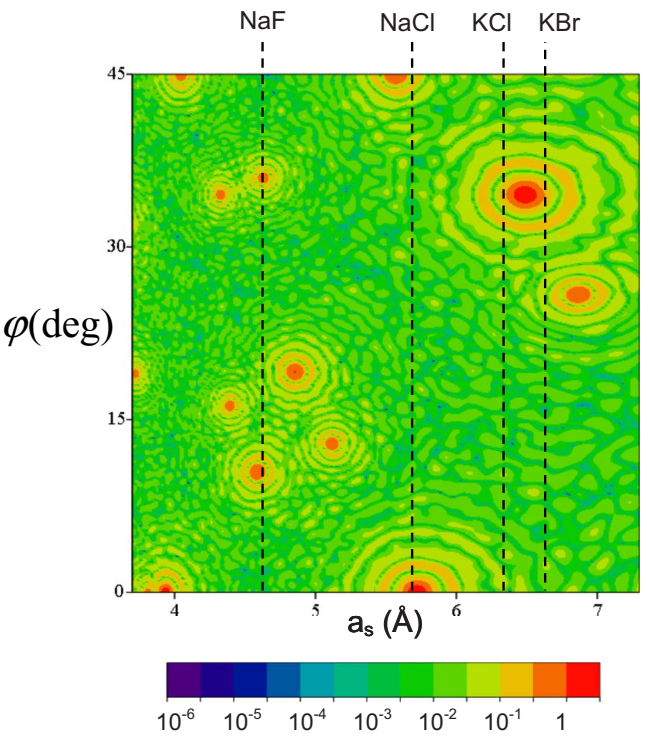

FIG. 4. (Color online) Stability diagram for PSP platelets on alkali halogenide (001) surfaces, shown as a logarithmic contour plot of the superposition of the generalized metrics $C(\varphi)=C_{10}(\varphi)$, $C_{11}(\varphi)$, and $C_{20}(\varphi)$. Pronounced maxima are associated with the one-dimensional coincidence structures with $\varphi=0°$ for the lattice constant range 5.6–5.7 Å (H0) and φ around 34.5° for lattice constants between 6.3 Å and 6.5 Å (L0). The third maximum at 3.8 Å is below the smallest alkali halide lattice parameter (H0′). Additionally shown are maxima due to the higher Fourier components G_{11} and G_{20} of the corrugation superimposed onto the map. Dashed lines mark the lattice constants of the four substrates studied. Table II lists all identified favorable epitaxial orientations with the associated Fourier component of the corrugation.

Calculations were also performed for the higher Fourier components (21) and (22). The first low-symmetry Fourier component (21) is characterized by an eightfold star. The many maxima produced by the generalized metrics $C_{21}(\varphi)$ and similarly $C_{22}(\varphi)$ could not be correlated with any observed epitaxial orientations, including the unassigned phases U1 and U2 from Table I. This may indicate that the associated Fourier components are already too weak to cause epitaxial alignment. The semi-*ab-initio* potential by Celli *et al.*[23] confirms that the higher-order Fourier components of the adsorption potential should be indeed much weaker.

Figure 4 shows the complete stability diagram of PSP

TABLE II. List of optimum lattice matches from the generalized metrics $C_{hk}(\varphi)$. Calculations are based on a circular domain of about 1000 molecules.

Fourier component	a_{opt} [a] (Å)	φ_{opt} [b] (deg)	Observations[c]
G_{10}	3.94	0	
G_{10}	5.72	0	NaCl–H0
G_{10}	6.49	34.53	KCl, KBr–L0
G_{11}	4.04	45	
G_{11}	4.59	10.47	NaF–L45
G_{11}	4.85	19.15	
G_{11}	5.57	45	NaCl–H45
G_{20}	4.32	34.54	
G_{20}	4.39	16.21	
G_{20}	4.63	36.00	NaF–L0
G_{20}	5.12	12.92	
G_{20}	6.87	25.85	

[a]Accuracy of lattice constant grid: 0.01 Å.
[b]Accuracy of angular grid: 0.01°.
[c]Classification of orientations is defined in Table I.

platelets on square substrate lattices as a function of substrate lattice parameter and epitaxial rotation. A superposition of the metrics $C(\varphi)=C_{10}(\varphi)$, $C_{11}(\varphi)$, and $C_{20}(\varphi)$ was plotted logarithmically in order to enhance the visibility of the finer structural details. The lattice constants of the substrates studied were indicated by dashed lines. While maxima corresponding to close-to-perfect matches are on the order of 1, the values between maxima drop to below 10^{-3}, indicating truly incommensurate arrangements. We also observe that the maxima of the generalized metrics due to higher Fourier components of the corrugation are less extended than the first order. The numerical values for the predicted maxima at a_S and φ were compiled in Table II along with the corresponding Fourier component of the corrugation. In Fig. 5 we present the specific results of the generalized metrics for the four surfaces in questions.

As an independent and challenging test of our approach, we investigated the well-known fcc (111) on bcc (110) epitaxial system and reproduced the low-symmetry Kurdjumov-Sachs phase with a 5.3° rotation between lattices and the symmetric Nishiyama-Wasserman phase[33,34] with aligned high-symmetry directions ($\varphi=0°$). This lattice matching between dissimilar lattices constitutes the most complex problem studied in depth in atomic epitaxy and thus serves as a reference for molecular epitaxial alignment. The Kurdjumov-Sachs phase was found to be related to the first-order Fourier component (11) and the Nishiyama-Wasserman phase to the higher-order and high-symmetry components (02) and (20) of the corrugation potential and both phases were faithfully reproduced by our metric.

D. Accommodation of the remaining misfit

The stability diagram in Fig. 4 based on the generalized metrics shows specific maxima associated with an optimum

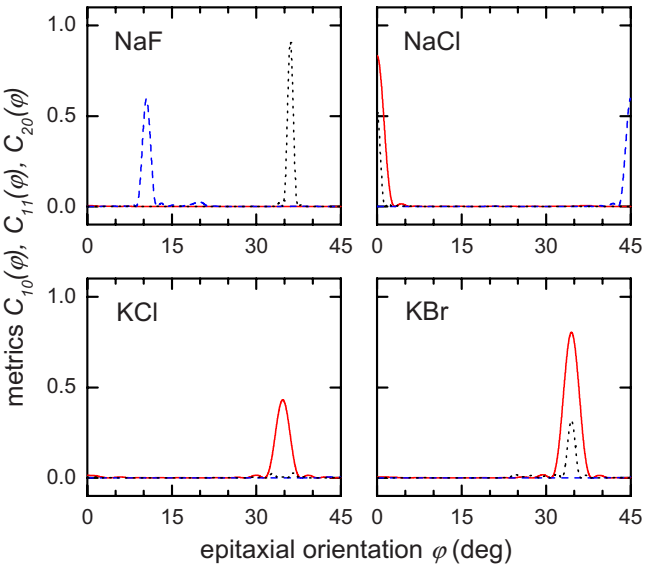

FIG. 5. (Color online) Predicted epitaxial orientations of PSP platelets on the four alkali halide (001) substrates studied. The respective substrates are indicated in each graph. The contributions of the three generalized metrics $C_{10}(\varphi)$ (red, solid line), $C_{11}(\varphi)$ (blue, dashed line), and $C_{20}(\varphi)$ (black, dotted line) are plotted, which are related to the lowest-order Fourier components of the surface corrugation function. Overall agreement with experimental data is to within better than 0.1°.

substrate lattice parameter and epitaxial rotation. However, it cannot be expected in general, that any real substrate will assume these specific values. So how is the remaining mismatch accommodated? First of all, we noticed in our calculations that the width of the maxima in the (a_s,φ) plane depends on the molecular domain size.[29,30] Thus lattice constant values close enough to a maximum will still provide a favorable epitaxial alignment. This is shown in Fig. 5, where the most significant generalized metrics are plotted at the lattice parameters of the four substrates.

This finite domain size may also relate to the classic studies of Frank and van der Merve, where they found that misfit is accommodated in an elastic adlayer by the formation of misfit dislocations.[33,35] This mechanism effectively limits the grain size, where a grain is now understood as the close to perfect region between dislocations. While our model does not include elastic deformation, choosing a small effective grain size emulates the more extended bands of stability found in elastic adlayer models.[36,37]

The metrics predict a slight rotation of the mismatched phases compared to the ideal geometric epitaxial rotation of the L0 phases of 34.535° for $a_{opt}=6.49$ Å, which is correlated with the molecular [110] rows being synchronized with and parallel to the principal substrate corrugation. The predicted φ values of 34.69° and 34.47° at the KCl and KBr lattice parameters, respectively, differ slightly from the optimum value for the L0 orientation. On the other hand, the experimentally observed values, 34.58° (KCl) and 34.50° (KBr) had smaller deviations from the optimum value than the predicted values. Note that this small angular deviation is also a function of domain size. The above values were calculated for a domain of 250 point contacts. Hence we state

here only qualitatively that the finite domain size may be accompanied with a slight angular deviation to alleviate the mismatch.

Symmetric adlayer rotations from high-symmetry substrate directions have been reported in rare gas layers on graphite and metal surfaces[38,39] and show pronounced epitaxial rotations of several degrees as a function of the adlayer density. Interactions in such systems are dominated by the substrate-adsorbate interaction, i.e., the adlayer is compressed by addition of atoms, before the next layer develops. The opposite holds for aromatic molecules such as PSP where the interaction of the π orbitals determines the packing density within the layers. Moreover PSP does not seem to form a wetting layer but shows pronounced three-dimensional Vollmer-Weber growth. As deviations of the PSP data from the epitaxial orientation values obtained within the rigid lattice approximation amount to only some 0.01° rather than degree-size rotations in rare gas layers, the Novaco-McTague mechanism[38] does not seem to apply.

IV. DISCUSSION

The good agreement of experimentally observed epitaxial orientation with the predictions from our method highlights the role of the surface corrugation, i.e., short-range repulsive interactions, for obtaining epitaxially aligned molecular crystals. Our model only considers the interaction of the terminal hydrogen atoms with the surface corrugation, but nonetheless we found that the generalized metrics $C_{hk}(\varphi)$ explain all pronounced preferential orientations of PSP on a series of alkali halide surfaces.

PSP is a member of an important class of rodlike aromatic molecules, in which the herringbone stacking inside close-packed molecular layers defines the molecular lattice, while epitaxial orientation is achieved by the terminal atoms in close contact with the substrate surface. This class of molecules includes the *para*-phenylenes, the oligothiophenes, and the oligoacenes, which have received much attention in the organic electronics community with regard to applications in organic light-emitting devices and thin-film transistors.

PSP platelets on rocksalt-type surfaces can also be regarded as an ideal model system. The molecule has a simple rodlike shape consisting of six coplanar phenyl rings connected by single bonds. The molecule-molecule interaction within the molecular layers appears to dominate the adsorbate-substrate interaction, as evidenced by the observed structure of the platelets[5] which is indistinguishable from the bulk structure. In addition the alkali halide cleavage surfaces are atomically well defined, chemically inert, and non reactive. Hence this system constitutes an ideal case of van der Waals epitaxy.[40,41]

The problem of analyzing preferential epitaxial orientations has its origins in the classic works of Frank and van der Merwe.[35] We note that the one-dimensional lattice match found for the H0 and H45 arrangements closely resembles the Nishiyama-Wasserman arrangement of an fcc (111) adlayer on a bcc (110) substrate[33,34] along high-symmetry azimuths. Simple model systems, such as rare gas adlayers on graphite, have been studied in great detail both experimentally and theoretically in the past.[39] Grey and Bohr[29] emphasized the role of domain shape and finite-size effects stabilizing epitaxial structures which was further extended in Monte Carlo simulations by Vives and Lindgård.[30] We mention that this domain-shape effect is reproduced by our metric.

Ward and co-workers[31,32] undertook extensive calculations of favorable epitaxial arrangements in molecular adlayers based on model potentials for molecules on nonreactive solid substrates. Among their methods, they also investigated a simplified approach based on a first-order formal Fourier expansion of the adatom potential.[31,32] Based on their extensive simulations Ward and co-workers[32] proposed a classification scheme for molecular epitaxy.

Recently, another epitaxy mode was reported[42] extending this classification. The latter so-called line-on-line mode seems to correspond to the PSP epitaxial orientations observed, where the $(20\bar{3})$ or $(11\bar{1})$ PSP reflections are lined up along the same lateral direction as the (220) and (200) reflections of the substrates. We could show that in the case of PSP this epitaxy mode seems to be favored because rows of molecules lock in with the main Fourier components of the surface corrugation. We also observed that the corrugation match worked only along one direction, while the perpendicular direction can be considered incommensurate.

An attractive feature of the simple metric introduced in Sec. III B is that for the high-symmetry (001) surfaces and a well-defined plane of point contacts of the molecular crystallites predictions of preferential epitaxial orientations can be made solely based on the lattice constants and the symmetry of substrate, i.e., without knowledge of the detailed potential parameters. By including higher Fourier components in form of generalized metrics $C_{hk}(\varphi)$, we were able to classify most of the dominant preferential orientations of PSP platelets on alkali halide substrates spanning a lattice constant range from 4.6 to 6.6 Å.

The metrics $C_{hk}(\varphi)$ provided us also with the means to systematically identify all favorable epitaxial alignments induced by the substrate corrugation. Moreover, the metrics predict additional preferential orientations that may be relevant for other rocksalt-type substrates, such as LiF (lattice parameter 4.02 Å), MgO (4.21 Å), CaO (4.81 Å), LiCl (5.13 Å), and KI (7.07 Å). Studies of surfaces such as KF (5.35 Å) could also be interesting, in which the lattice parameter does not coincide with maxima in the stability diagram in Fig. 4, and therefore may reveal other Fourier components of the molecule-surface interaction.

The only prominent structure which defied explanation within out method was the L0 structure on NaCl (001). Specifically, the L0 phase on NaCl (001) is not favored by a good match with any maxima in the stability diagram. The L0 phase has a peculiar appearance with sharp peaks superimposed on a broad distribution. The broad distribution would be consistent with our expectation. It is conceivable that the sharp L0 peaks are due to growth of PSP on another type of PSP crystallite. It should be noted that NaCl (001) features the highest abundance of epitaxial orientations among the four substrate studied and is the only surface fa-

voring also the symmetric arrangement with PSPs *a* and *b* along the substrate high-symmetry directions. This may be related to the PSP platelet on the NaCl (001) lattice being close to a transition point where the molecular rows switch alignment from parallel to the substrate [110] direction, characteristic for KCl (001), KBr (001) with PSP L0 crystallites, to [100], as for NaF (001) with PSP L45 crystallites.

Similarly the generalized metrics did not provide an explanation for the additional phases U1 and U2 on the NaF, NaCl, and KCl substrates, which show up as minor, but reproducible maxima in the pole figure scans. This may either be an indication of a different alignment mechanism or that these phases form on top of other material. Note that all unassigned peaks have the scattering vector $(20\bar{3})$ of the PSP bulk phase are thus most likely associated with PSP crystallites. Further studies in this range of substrate lattice constants as well as a more extended set of pole figure scans would be highly desirable in order to pin down the orientation mechanism.

It needs to be stressed that our approach is well suited for situations, where specific atoms within a molecule interact with the substrate corrugation. Our method is not applicable in cases where extended π systems interact with the substrate, e.g., for large planar aromatics lying on a substrate, for which full potentials are needed.[31,32] Nonetheless, our method can be applied to a number of important cases of molecular absorption and provides a link to the bulk of earlier work on atomic epitaxy.

V. SUMMARY

Physisorbed molecular films on nonreactive substrates form a technologically interesting and scientifically rich class of absorption systems.[1–17] We presented detailed data for the simple model system of PSP platelets grown on a variety of alkali halide surfaces, which revealed a surprising amount of complexity. We introduced a set of simple metrics $C_{hk}(\varphi)$ based solely on lattice parameters and basic symmetry considerations of the epitaxial potential. Using these metrics, we were able to classify most types of the observed complex epitaxial alignments and identify the substrate corrugation, acting on the PSP terminal hydrogen atoms in close contact to the substrate, as the driving force.

ACKNOWLEDGMENTS

We are deeply indebted to James G. Skofronick, Florida State University, for his long-standing support and encouragement for these systematic growth studies. We learned a great deal about atom-surface interactions from E. Hulpke, R. Vollmer, D. Eichenauer, and J. P. Toennies at the Max-Planck-Institut für Strömungsforschung in Göttingen, Germany. Special thanks to J. R. Manson, Clemson University, and George G. Malliaras, Cornell, for their remarks and encouragement at an early stage of these studies. We thank Dave Nowak, Cornell, for his help in setting up the G2 kappa diffractometer. We thank Darren Dale, Cornell, for critical reading and commenting on the paper. Funding of this work at Florida State University was provided by NSF under Grants No. DMR-0114094 and No. DMR-0216881 as well as by (U.S.) DOE under Contract No. DE-AC05-960R22464 and NSF Award No. DMR-0086210. This work was based upon research conducted at the Cornell High Energy Synchrotron Source (CHESS) which was supported by the National Science Foundation and the National Institutes of Health/National Institute of General Medical Sciences under NSF Award No. DMR-0225180.

APPENDIX A: EVALUATION OF LATTICE SUMS

The substrate in-plane reciprocal lattice vector $\boldsymbol{G}_{hk}$ can be written as

$$\boldsymbol{G}_{hk} = \frac{2\pi}{a_S}(hk),$$

with a_S being the substrate surface lattice constant. The rotated lattice vector of molecule (mn) can be expressed as

$$\boldsymbol{R}_{mn}(\varphi) = \begin{pmatrix} \cos(\varphi) & -\sin(\varphi) \\ \sin(\varphi) & \cos(\varphi) \end{pmatrix} \begin{pmatrix} ma \\ nb \end{pmatrix},$$

with the lattice constants a,b of the rectangular molecular lattice. The scalar product of both vectors yields

$$\boldsymbol{G}_{hk} \cdot \boldsymbol{R}_{mn}(\varphi) = 2\pi \left\{ h\left[m\frac{a}{a_S}\cos(\varphi) - n\frac{b}{a_S}\sin(\varphi) \right] + k\left[m\frac{a}{a_S}\sin(\varphi) + n\frac{b}{a_S}\cos(\varphi) \right] \right\}.$$

We introduce the functions

$$xc_h(\varphi) = 2\pi h\frac{a}{a_S}\cos(\varphi),$$

$$xs_k(\varphi) = 2\pi k\frac{a}{a_S}\sin(\varphi),$$

$$yc_k(\varphi) = 2\pi k\frac{b}{a_S}\cos(\varphi),$$

$$ys_h(\varphi) = -2\pi h\frac{b}{a_S}\sin(\varphi),$$

and obtain a form suitable for evaluation of the lattice sum at given epitaxial rotation φ:

$$\mathbf{G}_{hk} \cdot \mathbf{R}_{mn}(\varphi) = \{m[xc_h(\varphi) + xs_k(\varphi)] + n[yc_k(\varphi) + ys_h(\varphi)]\}.$$

In the following we will have to evaluate lattice sums of the form

$$\sum_{\mathrm{star}\{\boldsymbol{G}_{hk}\}} \sum_{(m,n)\in \mathrm{domain}} \exp(i\boldsymbol{G}_{hk}\boldsymbol{R}_{mn}).$$

The star of $\mathbf{G}_{hk}$ contains all symmetry-equivalent vectors of $\mathbf{G}_{hk}$. In particular, $\mathbf{G}_{-h,-k}=-\mathbf{G}_{hk}$ is always contained. The sum over such Friedel pairs (hk) and $(-h,-k)$ yields

TABLE III. Epitaxial matrices of prominent epitaxial alignments.

Substrate	Phase	Epitaxial matrix
NaF	L45	$\begin{pmatrix} 2.425 & 0.448 \\ -0.306 & 1.659 \end{pmatrix}$
NaCl	H45	$\begin{pmatrix} 1.432 & 1.432 \\ -0.98 & -0.98 \end{pmatrix}$
KCl	L0	$\begin{pmatrix} 1.498 & 1.032 \\ -0.706 & 1.025 \end{pmatrix}$
KBr	L0	$\begin{pmatrix} 1.429 & 0.982 \\ -0.672 & 0.977 \end{pmatrix}$

$$\exp(iG_{hk}R_{mn}) + \text{c.c.} = 2\cos(G_{hk}R_{mn}).$$

Now we are ready to perform the sum over a molecular domain,

$$s_{hk} = \sum_{(m,n)\in \text{domain}} \cos\{m[xc_h(\varphi) + xs_k(\varphi)] + n[yc_k(\varphi) + ys_h(\varphi)]\}.$$

For the summation over the star of $\mathbf{G}_{hk}$ we have to distinguish the following three cases:

$$(h0):\ h > 0, \quad k = 0,$$

$$(hh):\ h = k > 0,$$

$$(hk):\ h,k > 0, \quad k \neq h.$$

Thus we obtain for the generalized metrics $C_{hk}(\varphi)$ for the higher Fourier components of the corrugation:

$$C_{h0}(\varphi) = \{s_{h0}(\varphi) + s_{0h}(\varphi)\}^2,$$

$$C_{hh}(\varphi) = \{s_{hh}(\varphi) + s_{h,-h}(\varphi)\}^2,$$

$$C_{hk}(\varphi) = \{s_{hk}(\varphi) + s_{h,-k}(\varphi) + s_{kh}(\varphi) + s_{k,-h}(\varphi)\}^2.$$

The centered rectangular molecular lattice unit cell contains two terminal hydrogen atoms at positions (0,0) and $(a/2,b/2)$. Lattice sums have to be evaluated for each site and then added.

APPENDIX B: EPITAXIAL MATRICES

Epitaxial relationships can also be described in form of epitaxial matrices $\boldsymbol{M}$. If the surface lattice constants of the substrate and film are given by $\boldsymbol{a}_S$, $\boldsymbol{b}_S$, and $\boldsymbol{a}_F$, $\boldsymbol{b}_F$, respectively, then the epitaxial matrix $\boldsymbol{M}=(m_{i,k})$ with $i,k=1,2$ is defined as

$$\boldsymbol{a}_F = m_{11}\boldsymbol{a}_S + m_{12}\boldsymbol{b}_S,$$

$$\boldsymbol{b}_F = m_{21}\boldsymbol{a}_S + m_{22}\boldsymbol{b}_S.$$

In the case of PSP on the fcc (100) surface of alkali halide surfaces, these matrices can be derived easily from the preferred orientation angles φ. First we note that the substrate surfaces form square lattices with lattice constants a_S, as introduced in Sec. II. The [110] direction coincides with the [10] direction of the surface unit cell, and φ is measured relative to this direction. The PSP surface lattice is centered rectangular with lattice constants a and b, as introduced in Sec. II. Thus for this simple case of two rectangular lattices the epitaxial matrices $\boldsymbol{M}$ are given by

$$\boldsymbol{M} = \frac{1}{a_S}\begin{pmatrix} a_F\cos(\phi) & a_F\sin(\phi) \\ -b_F\sin(\phi) & b_F\cos(\phi) \end{pmatrix}.$$

Due to the multitude of observed epitaxial alignments compiled in Table I, we will only provide the most prominent orientational phase for each substrate for illustration (Table III).

*Corresponding author. dms79@cornell.edu

[1] G. Malliaras and R. H. Friend, Phys. Today **58** (5), 53 (2005).
[2] H. Yanagi and S. Okamoto, Appl. Phys. Lett. **71**, 2563 (1997).
[3] T. Mikami and H. Yanagi, Appl. Phys. Lett. **73**, 563 (1998).
[4] Y. Yoshida, H. Takiguchi, T. Hanada, N. Tanigaki, E.-M. Han, and K. Yase, J. Cryst. Growth **198-199**, 923 (1999).
[5] D.-M. Smilgies, N. Boudet, and H. Yanagi, Appl. Surf. Sci. **189**, 24 (2002).
[6] A. Andreev, R. Resel, D.-M. Smilgies, H. Hoppe, G. Matt, H. Sitter, N. S. Sariciftci, D. Meissner, H. Plank, and O. Zrzavecka, Synth. Met. **138**, 59 (2003).
[7] E. J. Kintzel, Jr., D.-M. Smilgies, J. G. Skofronick, S. A. Safron, and D. H. Van Winkle, J. Vac. Sci. Technol. A **22**, 107 (2004).
[8] A. Yu. Andreev, C. Teichert, G. Hlawacek, H. Hoppe, R. Resel, D.-M. Smilgies, H. Sitter, and N. S. Sariciftci, Org. Electron. **5**, 23 (2004).
[9] N. Yoshimoto, T. Sato, Y. Saito, and S. Ogawa, Mol. Cryst. Liq. Cryst. (Phila. Pa.) **425**, 1 (2004).
[10] T. Haber, A. Andreev, A. Thierry, H. Sitter, M. Oehzelt, and R. Resel, J. Cryst. Growth **284**, 209 (2005).
[11] E. J. Kintzel, Jr., D.-M. Smilgies, J. G. Skofronick, S. A. Safron, and D. H. Van Winkle, J. Cryst. Growth **289**, 345 (2006).
[12] T. Haber, M. Oehzelt, A. Andreev, A. Thierry, H. Sitter, D.-M. Smilgies, B. Schaffer, W. Grogger, and R. Resel, J. Nanosci. Nanotechnol. **6**, 698 (2006).
[13] H. Sitter, A. Andreev, Ch. Teichert, G. Hlawacek, T. Haber, D.-M. Smilgies, R. Resel, A. M. Ramil, and N. S. Sariciftci, Phys. Status Solidi B **242**, 1877 (2005); R. Resel, J. Phys.: Condens. Matter **20**, 184009 (2008).
[14] K. N. Baker, A. V. Fratini, T. Resch, H. C. Knachel, W. W. Adams, E. P. Socci, and B. L. Farmer, Polymer **34**, 1571 (1993).
[15] D. E. Nowak, D. R. Blasini, A. M. Vodnick, B. Blank, M. W. Tate, A. Deyhim, D.-M. Smilgies, H. Abruña, S. M. Gruner, and S. P. Baker, Rev. Sci. Instrum. **77**, 113301 (2006).

[16] E. J. Kintzel, Jr., D.-M. Smilgies, J. G. Skofronick, S. A. Safron, D. H. Van Winkle, T. W. Trelenberg, E. A. Akhadov, and F. A. Flaherty, J. Vac. Sci. Technol. A **19**, 1270 (2001).
[17] S. R. Forrest, Chem. Rev. (Washington, D.C.) **97**, 1793 (1997).
[18] T. Haber, R. Resel, A. Andreev, M. Oehzelt, D.-M. Smilgies, and H. Sitter (unpublished).
[19] A. Hoshino, S. Isoda, K. Kurato, and T. Kobayashi, J. Appl. Phys. **76**, 4113 (1994).
[20] J. E. Lennard-Jones and A. F. Devonshire, Proc. R. Soc. London, Ser. A **158**, 242 (1937).
[21] G. Wolken, Jr., J. Chem. Phys. **58**, 3047 (1973).
[22] G. Armand and J. R. Manson, Surf. Sci. **119**, L299 (1982).
[23] V. Celli, D. Eichenauer, A. Kaufhold, and J. P. Toennies, J. Chem. Phys. **83**, 2504 (1985).
[24] D. Eichenauer and J. P. Toennies, Surf. Sci. **197**, 267 (1988).
[25] P. W. Fowler and J. M. Hutson, Phys. Rev. B **33**, 3724 (1986).
[26] A. Frigo, F. Toigo, M. W. Cole, and F. O. Goodman, Phys. Rev. B **33**, 4184 (1986).
[27] D. J. Riley, A. P. Jardine, S. Dworski, G. Alexandrowicz, P. Fouquet, J. Ellis, and W. Allison, J. Chem. Phys. **126**, 104702 (2007).
[28] U. Garibaldi, A. C. Levi, R. Spadacini, and G. E. Tommei, Surf. Sci. **48**, 649 (1975).
[29] F. Grey and J. Bohr, Europhys. Lett. **18**, 717 (1992).
[30] E. Vives and P. A. Lindgård, Phys. Rev. B **47**, 7431 (1993).
[31] A. C. Hillier and M. D. Ward, Phys. Rev. B **54**, 14037 (1996).
[32] D. E. Hooks, T. Fritz, and M. D. Ward, Adv. Mater. **13**, 227 (2001).
[33] E. Bauer and J. H. van der Merwe, Phys. Rev. B **33**, 3657 (1986).
[34] R. Ramirez, A. Rahman, and I. K. Schuller, Phys. Rev. B **30**, 6208 (1984).
[35] F. C. Frank and J. H. van der Merwe, Proc. R. Soc. London, Ser. A **198**, 205 (1949); **198**, 216 (1949); **200**, 125 (1949).
[36] L. C. A. Stoop and J. H. van der Merwe, Thin Solid Films **94**, 341 (1982).
[37] A. Zangwill, *Physics at Surfaces* (Cambridge University Press, Cambridge, England, 1988), Chap. 16.
[38] A. D. Novaco and J. P. McTague, Phys. Rev. Lett. **38**, 1286 (1977).
[39] K. Kern, Phys. Rev. B **35**, 8265 (1987).
[40] A. Koma and K. Yoshimura, Jpn. J. Appl. Phys. **22**, L173 (1983).
[41] L. T. Vinh, M. Eddrief, J. E. Mahan, A. Vantomme, J. H. Song, and M.-A. Nicolet, J. Appl. Phys. **81**, 7289 (1997).
[42] S. C. B. Mannsfeld, K. Leo, and T. Fritz, Phys. Rev. Lett. **94**, 056104 (2005); S. C. B. Mannsfeld and T. Fritz, Phys. Rev. B **71**, 235405 (2005).